AIP | Journal of Applied Physics

Annealing temperature and thickness dependence of magnetic properties in epitaxial L10-Mn1.4Ga films

Y. H. Zheng, G. C. Han, H. Lu, and K. L. Teo

Citation: Journal of Applied Physics **115**, 043902 (2014); doi: 10.1063/1.4862172
View online: http://dx.doi.org/10.1063/1.4862172
View Table of Contents: http://scitation.aip.org/content/aip/journal/jap/115/4?ver=pdfcov
Published by the AIP Publishing

Annealing temperature and thickness dependence of magnetic properties in epitaxial $L1_0$-$Mn_{1.4}Ga$ films

Y. H. Zheng,[1,a)] G. C. Han,[2] H. Lu,[1] and K. L. Teo[1]
[1]*Department of Electrical and Computer Engineering, National University of Singapore, Singapore 117576*
[2]*Data Storage Institute, 5 Engineering Drive 1, Singapore 117608*

(Received 5 December 2013; accepted 1 January 2014; published online 22 January 2014)

$Mn_{1.4}Ga$ films with high perpendicular magnetic anisotropy and high crystalline quality were grown on MgO substrates with Cr buffer layer using molecular beam epitaxy. The crystalline structure and the surface morphology of the films have been systematically investigated as functions of *in-situ* annealing temperature (T_a) and film thickness. It is found that the magnetic properties can be largely tuned by adjusting T_a. As T_a increases, both saturation magnetization (M_s) and uniaxial perpendicular magnetic anisotropy constant (K_u) increase to the maximum values of 612 emu/cc and 18 Merg/cc at 300 °C, respectively, and then decrease. The morphology also changes with T_a, showing a minimum roughness of 2.2 Å at $T_a = 450$ °C. On the other hand, as the thickness increases, M_s and K_u increase while coercivity decreases, which indicates there is a magnetic dead layer with a thickness of about 1.5 nm at the interfaces. The detailed examination on the surface morphology of the films with various thicknesses shows a complicated film growth process, which can be understood from the relaxation mechanism of the interfacial strain.
 [http://dx.doi.org/10.1063/1.4862172]

INTRODUCTION

Ferromagnetic thin films with perpendicular magnetic anisotropy (PMA) have attracted considerable interests in advanced spintronic applications as they can be developed to overcome the superparamagnetic limit and enhance the thermal stability for ultrahigh-density magnetic storage devices.[1–3] In particular, the PMA materials with low saturation magnetization (M_s), small damping coefficient (α), and high spin polarization (P) are highly desirable for spin-transfer-torque magnetoresistive random access memory (STT-MRAM) as to realize high density and high writing speed.[4–6] Noble-metal-based FePt and FePd are the well-known ferromagnetic alloys exhibiting high PMA in $L1_0$ phase.[1,7–11] However, large α and high-temperature (>500 °C) annealing process to form $L1_0$ ordering in FePt and FePd thin films would suppress their applications in STT-MRAM. Recently, it has been shown that Mn_xGa ($1 \leq x \leq 3$) alloys in $L1_0$ or $D0_{22}$ phase have small α, low M_s, high P, and high PMA, which perfectly meet the requirements for STT-MRAM.[12–27] In addition, these Mn_xGa alloys are also promising for applications in ultrahigh-density perpendicular magnetic recording, permanent magnets, and magnetic domain wall race track memory.[24,28]

$L1_0$ phase is a thermodynamically stable phase for the Mn_xGa with x ranging from 1.15 to 1.89.[12,27] The first principle calculation shows that MnGa in $L1_0$ phase has an α as small as 0.0003, a P as high as 71%, and a $K_u > 26$ Merg/cc.[15,24,29] Experimentally, high PMA are obtained in molecular beam epitaxy (MBE) or magnetron sputtering deposited $L1_0$-Mn_xGa thin films with x ranging from 1.2 to 1.6.[18,20] In this study, $Mn_{1.4}Ga$ films were deposited by MBE. The structural and magnetic properties were tuned by varying the *in-situ* annealing temperatures (T_a) in order to obtain high crystalline quality, smooth surface, and high PMA. The thickness dependence of $Mn_{1.4}Ga$ film was also investigated in order to understand the interface effect and the origin of PMA in this material.

EXPERIMENT

$Mn_{1.4}Ga$ films were deposited on MgO (100) substrates with a Cr buffer layer in an ultrahigh vacuum MBE chamber. Before depositing $Mn_{1.4}Ga$ film, MgO substrate was annealed at 600 °C. A 40 nm thick Cr buffer layer was deposited at room temperature and subsequently *in-situ* annealed at 500 °C. After this heat treatment, a smooth surface with a root-mean-square (rms) of as low as 1.7 Å is obtained. The $Mn_{1.4}Ga$ layer was then deposited at room temperature and subsequently *in-situ* annealed at temperature T_a ranging from 100 to 450 °C. The film stack was finally capped with Ag layer of 4 nm at room temperature to prevent oxidation. The composition of the films was controlled by changing the fluxes of Mn and Ga effusion cells. After deposition, the composition $x = 1.4$ was further confirmed by both x-ray photoelectron spectroscopy (XPS) and inductively coupled plasma mass spectrometry (ICP-MS) measurements. The surface morphology was measured by an atomic force microscopy (AFM), and crystalline structural analysis was performed by x-ray diffractometer (XRD). Magnetization measurements were carried out using an alternating gradient magnetometer (AGM) and physical properties measurement system (PPMS).

RESULT AND DISCUSSION

Figure 1(a) shows XRD $\theta/2\theta$ patterns of 40 nm thick $Mn_{1.4}Ga$ films annealed with different T_a. The Cr (002), MnGa (002), and MnGa (001) peaks can be clearly observed, which

a)Electronic mail: elezheng@nus.edu.sg

indicates the films are grown along the *c*-axis. No secondary phase is found from the XRD patterns except for the film with $T_a = 450\,^{\circ}C$, where an additional broad peak is found at 61.25°, which can be ascribed to the (110) $L1_0$-MnGa peak from some misaligned MnGa grains.[19] Since the $\theta/2\theta$ XRD patterns of $D0_{22}$ and $L1_0$ crystal structures are quite similar, XRD ϕ scans were measured to identify the structure of the $Mn_{1.4}Ga$ films. As shown in Figure 1(b), the fourfold $L1_0$ {111} peaks are clearly observed. There is no $D0_{22}$ {011} peak present which is actually forbidden in $L1_0$ structure. This clearly indicates that $Mn_{1.4}Ga$ film is of $L1_0$ phase ordering. The ϕ scans of MgO {022}, Cr {022}, and MnGa {022} peaks were also measured to check the epitaxial relationship. As shown in Figure 1(c), the epitaxial relationship MgO(001)[100]//Cr(001)[110]//MnGa(001)[100] is achieved.

Figure 1(d) shows the lattice parameters obtained from XRD results. The in-plane lattice parameter *a* is calculated from *c* and interplanar spacing of MnGa (022) planes, which is obtained from the 2θ value of MnGa (022) peak. At $T_a = 100\,^{\circ}C$, the values of *a* and *c* are close to the bulk values ($a = 3.88$ Å, $c = 3.69$ Å).[12,13] However, as T_a increases, *a* increases while *c* decreases. This behavior relates to the strain in epitaxial $Mn_{1.4}Ga$ film for the lattice mismatch. Based on the epitaxial relationship Cr(001)[110]//MnGa(001)[100], an in-plane rotation is needed for $Mn_{1.4}Ga$ to follow Cr lattice. The lattice of $Mn_{1.4}Ga$ would contract along *c*-axis for the different values of the unit cells along $Mn_{1.4}Ga$ [100] (3.88 Å) and Cr [110] (4.07 Å), leading to a tensile strain in $Mn_{1.4}Ga$. The strain increases with the enhancement of crystalline structure when T_a increases.

We note that the T_a-induced *a* and *c* variations are different from the previously reported for case for $Mn_{2.5}Ga$ film deposited on Cr-buffered MgO substrates by magnetron sputtering. The *a* is nearly a constant and *c* decreases slightly with increasing T_a.[25] A possible reason is that the tensile strain in $Mn_{1.4}Ga$ films is larger than that in $Mn_{2.5}Ga$ film due to its larger lattice mismatch (4.67% for $L1_0$-MnGa and 3.96% for bulk $D0_{22}$-$Mn_{2.5}Ga$). The *c*/*a* ratio for the film with $T_a = 450\,^{\circ}C$ is 0.912, which is much smaller than the bulk value of 0.951, indicating a strong distortion of tetragonal lattice for the large tensile strain. As shown in Figure 1(e), the full width at half maximum (FWHM) from XRD rocking curves decreases as T_a increases, indicating the enhancement in the crystalline quality with high T_a. Figure 1(f) shows T_a dependence of surface roughness (R_q). For most T_a, R_q is small with a value from 2.2 to 3.9 Å except for the film with $T_a = 200\,^{\circ}C$, where R_q jumps to the maximum value of 8.0 Å. The trend of R_q dependence on T_a is quite different from that reported for the $Mn_{2.1}Ga$ films with $D0_{22}$ ordering.[23] There R_q increases monotonically with T_a, with an opposite trend of FWHM. Thus, the film with a high crystalline quality usually shows a large R_q, which is not favorable for device application such as magnetic tunnel junctions (MTJs). In our case, the $L1_0$-$Mn_{1.4}Ga$ film with high crystalline quality (FWHM = 0.42°) and smooth surface ($R_q = 2.2$ Å) can be obtained at $T_a = 450\,^{\circ}C$.

Figure 2(a) depicts *M*-*H* loops as a function of T_a with the magnetic field applied perpendicular to the film plane. At $T_a = 200\,^{\circ}C$, the loop shows two magnetic phases. For $T_a \geq 250\,^{\circ}C$, all the *M*-*H* loops are of rectangle shape,

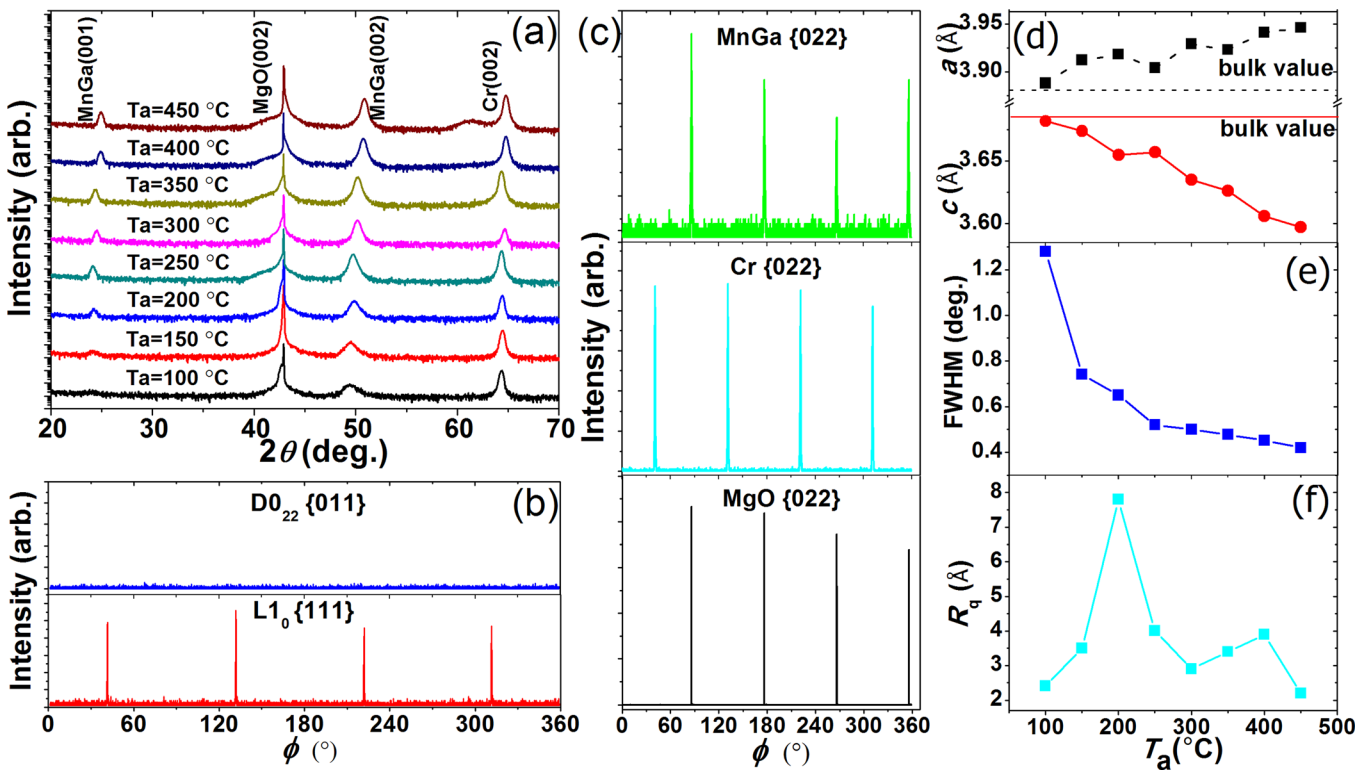

FIG. 1. (a) XRD $\theta/2\theta$ patterns of $Mn_{1.4}Ga$ films with different T_a; (b) ϕ scans for a $Mn_{1.4}Ga$ film; (c) ϕ scans of {022} peaks for $Mn_{1.4}Ga$/Cr/MgO heteroepitaxial structure; (d) Lattice parameters (bulk values of lattice parameters for $Mn_{1.4}Ga$ are also indicated with black dashed line and red solid line); (e) FWHM; (f) R_q dependence on T_a for $Mn_{1.4}Ga$ films.

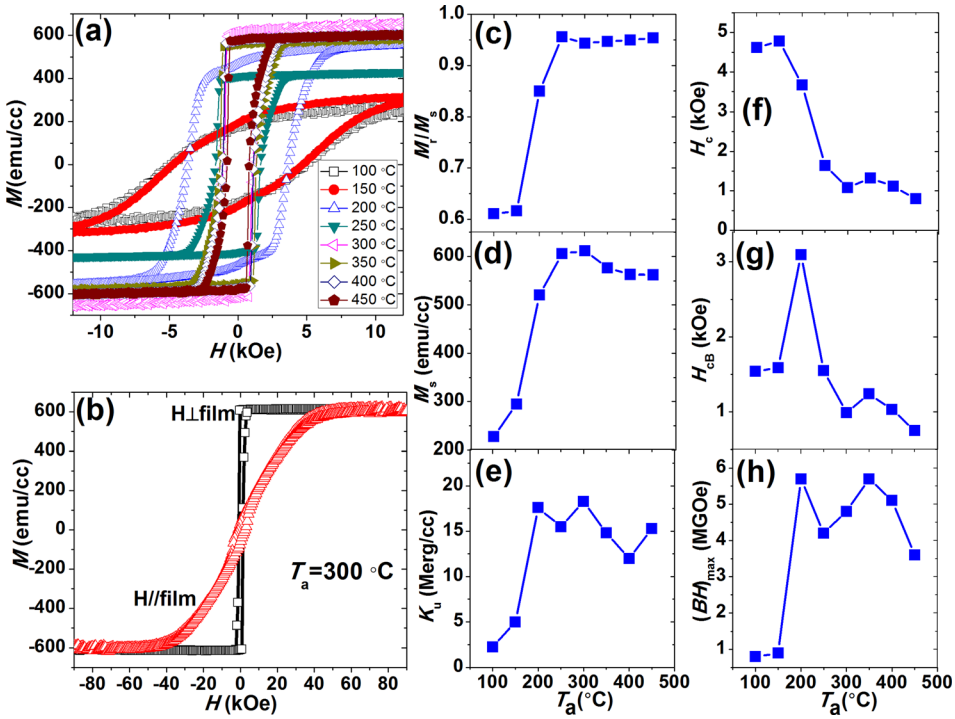

FIG. 2. (a) Hysteresis loops measured at 300 K with the magnetic field applied perpendicular to the film plane for $Mn_{1.4}Ga$ films; (b) Hysteresis loops measured at 300 K for the $Mn_{1.4}Ga$ film with $T_a = 300\,^{\circ}C$; (c) M_r/M_s, (d) M_s, (e) K_u, (f) H_c, (g) H_{cB}, and (h) $(BH)_{max}$ as a function of T_a for $Mn_{1.4}Ga$ films.

indicating single magnetic phase in the film with the magnetization easy axis perpendicular to the plane. For comparison, Figure 2(b) shows typical *M-H* loops measured with magnetic fields applied perpendicular to the plane (open circles) and in-plane (open triangles) for the $Mn_{1.4}Ga$ film with $T_a = 300\,^{\circ}C$. One can see that the loops confirm the PMA of the film. The anisotropy constant K_u can be obtained from the relation

$$K_u = M_s H_k^{eff}/2 + 2\pi M_s^2, \quad (1)$$

where H_k^{eff} is the effective perpendicular magnetic anisotropy field. The value of H_k^{eff} can be estimated as the field at which the in-plane and the out-of-plane *M-H* loops merge. From Figure 2(b), the H_k^{eff} is 52 kOe and M_s is about 612 emu/cc, which give the value of K_u of 18 Merg/cc, which is comparable to that for $D0_{22}$-MnGa films. Figures 2(c)–2(f) give the key magnetic parameters as a function of T_a. High squareness $(M_r/M_s) \geq 0.94$, high K_u, and low H_c can be achieved with $T_a > 200\,^{\circ}C$, where M_r is the remnant magnetization. These results can be attributed to better crystalline quality with high T_a. It is noted that the M_s (~612 emu/cc) obtained in our experiments is higher than previously reported Mn_xGa films, although it is still lower than the theoretically predicted value of 845 emu/cc for stoichiometric $L1_0$-MnGa ($x = 1$).[18,24,29] As T_a increases, M_s increases to a saturation value of about 612 emu/cc at $T_a = 300\,^{\circ}C$. The slight decrease in M_s at $T_a > 300\,^{\circ}C$ may be related to the decrease in the lattice parameter *c* at high T_a. As reported by Wang *et al.*, the magnetic moment of a Mn atom can decrease by 0.23 μ_B (~47 emu/cc) when *c* decreases from 3.7 Å to 3.6 Å.[30] The larger decrease in *c* may be one of the reasons why the reported M_s of $Mn_{1.5}Ga$ film ($c = 3.47$ Å, $M_s = 190$ emu/cc) is much lower than ours.[24] The estimated K_u ranges from 12 to 18 Merg/cc for our $Mn_{1.4}Ga$ films with $T_a \geq 200\,^{\circ}C$, while only 2 to 5 Merg/cc for low T_a films.

Apart from spintronic application, rare-earth-free and noble-metal-free Mn_xGa alloys are also good candidates for permanent magnet application. The normal coercivity (H_{cB}) and magnetic energy product ($(BH)_{max}$) are key parameters for permanent magnets, where H_{cB} can be determined from the *B-H* curve. Figures 2(g) and 2(h) give the values of H_{cB} and $(BH)_{max}$ estimated from *B-H* curves as a function of T_a. The highest H_{cB} of 3.09 kOe is obtained at $T_a = 200\,^{\circ}C$, while the highest $(BH)_{max}$ of 5.75 MGOe is achieved at $T_a = 350\,^{\circ}C$. This $(BH)_{max}$ value is larger than that reported in ferrite magnets[31] and Mn_xGa films on GaAs recently.[17,20]

The thickness dependence of $Mn_{1.4}Ga$ films was investigated by depositing six samples with thickness ranging from 5 nm to 100 nm at the same T_a of 300 °C. To directly investigate the morphology of $Mn_{1.4}Ga$ films, no Ag protection layers were deposited on these samples. Figure 3 shows their AFM images ($2 \times 2\,\mu m$ scan size). To reduce the influence of oxidation on morphology, the samples were immediately measured when they were taken out from the vacuum chamber. As marked by the black circles in Figure 3(a), several islands with the height of several nanometers appear on the surface of 5 nm thick $Mn_{1.4}Ga$ film. The islands grow larger and denser when the film thickness increases to 10 nm as shown in Figure 3(b). The width and height of the islands can be up to 240 nm and 12 nm, respectively. For thicker $Mn_{1.4}Ga$ films, the evolution of morphology with thickness (see Figures 3(c)–3(f)) is similar to that for Ge layer on Si(001) substrate reported by Hartmann *et al.*,[33] which is probably due to the similar lattice mismatch for these two systems (4.6% for $Mn_{1.4}Ga$/Cr and 4.2% for Ge/Si). Initially, ripples form with small spatial wavelengths, and then become longer in both width and length and finally forms a crosshatching pattern. Some pits with widths and heights about 70–120 nm and 1–4 nm also appears for films from 20 to 40 nm.

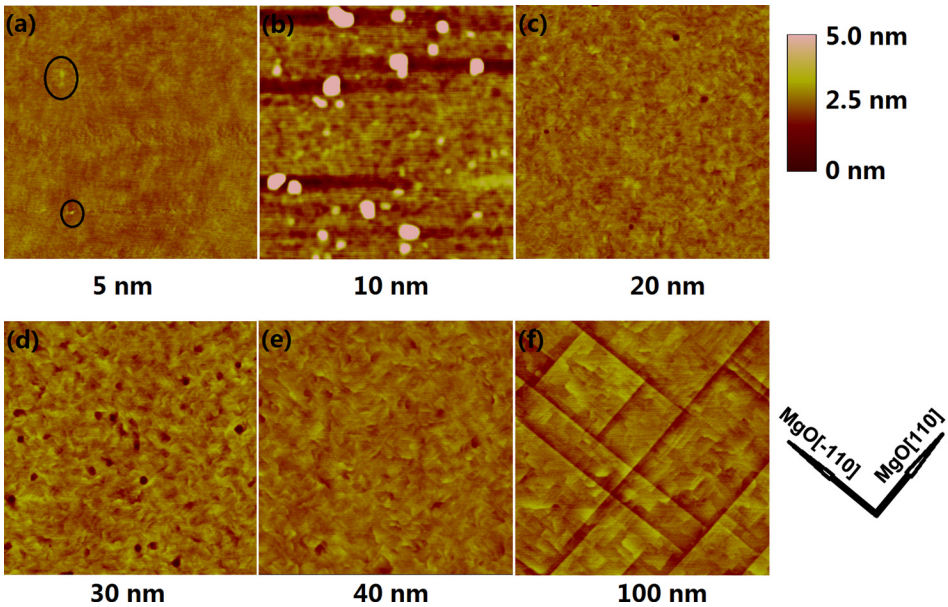

FIG. 3. AFM images ($2 \times 2\,\mu$m scan size) for $Mn_{1.4}Ga$ films annealing at 300 °C with different thickness (the lattice directions of MgO in all images are the same and labeled by the arrows in the bottom right corner).

Heteroepitaxial strained layers can relax by two competing mechanisms, namely, forming islands or pits on surface and forming misfit dislocations.[34] As for our films, the first mechanism is dominant for the large lattice mismatch (4.6%) when the film grown is not very thick. For thin films with thickness of less than 20 nm, islands are more easily formed through nucleation as the films are not thick enough to support pits formation.[34] As the thickness increases further, the formation of pits becomes more energetically favored, which can be seen clearly from Figures 3(c)–3(e). For thicker film, dislocations are also formed to relax the strain, which can influence the morphology too. Based on the model in Ref. 35, a misfit dislocation will create a strain field that causes lattice contraction in the (001) plane and expansion along ⟨001⟩ direction. The expansion will lead to the upward movement of the layers above the dislocation and form some ripples as shown in Figures 3(c)–3(e). The spatial wavelengths of ripples become wider and finally form a crosshatching pattern for the pile-up of the dislocations. Crosshatching lines are along $Mn_{1.4}Ga$ ⟨110⟩ (the same as MgO ⟨110⟩ labeled in Figure 3). They are caused by the misfit dislocations in $Mn_{1.4}Ga$/Cr interface instead of Cr/MgO interface because the latter ones were reported along Cr ⟨110⟩ (the same as MgO ⟨100⟩).[32] Compared to the normal crosshatching patterns for SiGe/Si, InGaAs/GaAs, and AlGaAs/GaAs heterostructures,[35] the crosshatching lines in our $Mn_{1.4}Ga$ films are short but dense. The reason is that the short misfit dislocations are easily formed for low temperature deposited $Mn_{1.4}Ga$ film.

It would be interesting to find the possible relations between dislocations and the formation of islands and pits.[36] Some islands and pits in Figures 3(b)–3(d) are approximately square in shape with two sides along the ⟨100⟩ directions of MgO substrate. This shows that the islands may relate to the threading dislocations originated from Cr/MgO interface, which are along MgO ⟨100⟩ direction.[32] Similarly, the pits with two sides along the MgO ⟨110⟩ directions may relate to the threading dislocations originated from $Mn_{1.4}Ga$/Cr interface.

Figure 4(a) shows the XRD patterns obtained for $Mn_{1.4}Ga$ films with various thickness at $T_a = 300$ °C. For all thicknesses ranging from 5 nm to 100 nm, the $L1_0$-MnGa (002) peak can be observed. The peak intensity increases as the thickness increases. For 10 nm and below, $Mn_{1.4}Ga$ (001) peak is not very clear, while for 100 nm, all $L1_0$-MnGa peaks from (001) to (003) are clearly seen. The lattice parameters a, c and FWHM are shown functions of thickness in Figure 4(b). FWHM decreases with thickness and reaches a minimum value of 0.39° at 100 nm. In contrast, Wu *et al.*[26] reported an opposite FWHM variation with thickness, i.e., FWHM increases with thickness for $D0_{22}$-ordered $Mn_{2.5}Ga$ films deposited by magnetron sputtering. The lattice parameters c increases while a decreases with thickness, indicating a strain relaxation behavior in the film. The rather small c in 5 nm thick film may result from the large tensile stress in the $Mn_{1.4}Ga$ film.

Figure 4(c) shows M-H loops as a function of film thickness with the magnetic field applied perpendicular to the plane. For 5 nm thick $Mn_{1.4}Ga$ film, the M-H loop is not square in shape, which may relate to the large tensile strain. However, for the films with thickness from 10 nm to 40 nm, square M-H loops are observed, indicating high PMA. When the thickness is increased to 100 nm, the M-H loop is characterized by the rather low M_r and the abrupt transitions in magnetization. This kind of loop can be found in relatively thick film with high PMA and is well understood in the model developed by Cape and Lehman.[37–39] At high magnetic field, all magnetic moments are oriented in the field direction and M begins to drop rapidly when H decreases to 1.3 kOe. This drop is associated with the nucleations of magnetic bubbles with opposite magnetization. By further decreasing H, the bubbles grow larger and the quasilinear decrease of M with H can be explained by the domain wall motion.[40]

Figures 4(d)–4(f) show M_s, K_u, and H_c as a function of thickness. Both M_s and K_u increase with thickness till 40 nm and slightly decrease with increasing thickness. This behavior is quite different from the reported $Mn_{1.86}Ga$ and

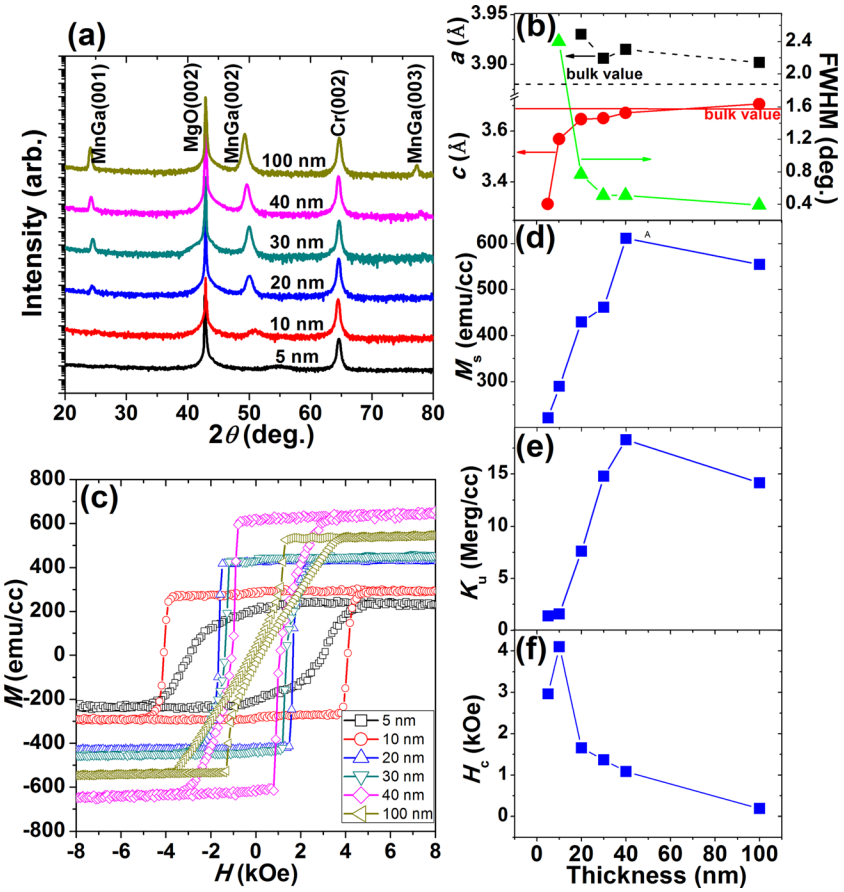

FIG. 4. (a) XRD $\theta/2\theta$ patterns of $Mn_{1.4}Ga$ films with $T_a = 300\,^{\circ}C$; (b) Lattice parameters (bulk values of lattice parameters for $Mn_{1.4}Ga$ are labeled (black dashed line and solid line)) and FWHM as a function of thickness for $Mn_{1.4}Ga$ films with $T_a = 300\,^{\circ}C$; (c) Hysteresis loops measured at 300 K for $Mn_{1.4}Ga$ films with $T_a = 300\,^{\circ}C$; (d) M_s, (e) K_u, and (f) H_c as a function of thickness for $Mn_{1.4}Ga$ films with $T_a = 300\,^{\circ}C$.

$Mn_{2.5}Ga$ films for which M_s is independent of thickness.[21,26] A possible reasons for the lower M_s in the thinner film is that there may be magnetic dead layers near the interface and the surface in view of symmetry breaking. From the data in Figure 4(d), the thickness of the dead layer in both interfaces (surface) is estimated to be ~1.5 nm. Thus, the improvement of interface quality is important to obtain high M_s and high K_u in the ultrathin films. Besides the magnetic dead layer at the interface or the surface, the smaller lattice constant c may be another possible reason for the lower M_s, which is already discussed in this report. Except for the 5 nm thick $Mn_{1.4}Ga$ film, H_c monotonically decreases with increasing thickness, which is mainly due to the increase of in-plane phase.

CONCLUSIONS

In summary, magnetic $Mn_{1.4}Ga$ films with high PMA and high crystalline quality were grown on MgO substrate via a Cr buffer layer using MBE. The $Mn_{1.4}Ga$ films with different T_a or thickness show M_s from 230 emu/cc to 612 emu/cc, K_u from 2 to 18 Meg/cc, H_c from 0.2 kOe to 4.6 kOe, $(BH)_{max}$ up to 5.7 MGOe. The detailed examination on the surface morphology of the films with various thicknesses shows a complicated film growth process, which can be understood from the relaxation mechanism of the interfacial strain.

ACKNOWLEDGMENTS

This work was supported by Singapore Agency for Science, Technology, and Research (A*STAR), under Grant No. 092 151 0087. The authors thank Dr. Ji Rong and Xie Huiqing at Data Storage Institute for their help with XPS and ICP-MS measurements. We also thank T. Kubota for helpful discussion.

[1]A. T. McCallum, P. Krone, F. Springer, C. Brombacher, M. Albrecht, E. Dobisz, M. Grobis, D. Weller, and O. Hellwig, Appl. Phys. Lett. **98**, 242503 (2011).
[2]M. Weisheit, S. Fähler, A. Marty, Y. Souche, C. Poinsignon, and D. Givord, Science **315**, 349 (2007).
[3]I. M. Miron, K. Garello, G. Gaudin, P. J. Zermatten, M. V. Costache1, S. Auffret, S. Bandiera, B. Rodmacq, A. Schuhl, and P. Gambardella, Nature **476**, 189 (2011).
[4]M. Nakayama, T. Kai, N. Shimomura, M. Amano, E. Kitagawa, T. Nagase, M. Yoshikawa, T. Kishi, S. Ikegawa, and H. Yoda, J. Appl. Phys. **103**, 07A710 (2008).
[5]S. Ikeda, K. Miura, H. Yamamoto, K. Mizunuma, H. D. Gan, M. Endo, S. Kanai, J. Hayakawa, F. Matsukura, and H. Ohno, Nature Mater. **9**, 721 (2010).
[6]D. C. Worledge, G. Hu, D. W. Abraham, J. Z. Sun, P. L. Trouilloud, J. Nowak, S. Brown, M. C. Gaidis, E. J. O'Sullivan, and R. P. Robertazzi, Appl. Phys. Lett. **98**, 022501 (2011).
[7]T. Shima, T. Moriguchi, S. Mitani, and K. Takanashi, Appl. Phys. Lett. **80**, 288 (2002).
[8]Y. C. Wu, L. W. Wang, and C. H. Lai, Appl. Phys. Lett. **93**, 242501 (2008).
[9]S. C. Chen, T. H. Sun, C. L. Chang, W. H. Su, C. L. Shen, and J. R. Chen, IEEE Trans. Magn. **47**, 524 (2011).
[10]D. Weller, A. Moser, L. Folks, M. E. Best, W. Lee, M. F. Toney, M. Schwickert, J. U. Thiele, and M. F. Doerner, IEEE Trans. Magn. **36**, 10 (2000).
[11]T. Shima, K. Takanashi, Y. K. Takahashi, and K. Hono, Appl. Phys. Lett. **85**, 2571 (2004).
[12]S. S. Lu, J. K. Liang, and Z. R. Yang, Acta. Phys. Sin. **28**, 54 (1979).
[13]M. Tanaka, J. P. Harbison, J. DeBoeck, T. Sands, B. Philips, T. L. Cheeks, and V. G. Keramidas, Appl. Phys. Lett. **62**, 1565 (1993).

[14]B. Balke, G. H. Fecher, J. Winterlik, and C. Felser, Appl. Phys. Lett. **90**, 152504 (2007); Phys. Rev. B **77**, 054406 (2008).
[15]S. Mizukami, F. Wu, A. Sakuma, J. Walowski, D. Watanabe, T. Kubota, X. Zhang, H. Naganuma, M. Oogane, Y. Ando, and T. Miyazaki, Phys. Rev. Lett. **106**, 117201 (2011).
[16]H. Kurt, K. Rode, M. Venkatesan, P. Stamenov, and J. M. D. Coey, Phys. Status Solidi B **248**, 2338 (2011); Phys. Rev. B **83**, 020405(R) (2011).
[17]L. J. Zhu, S. H. Nie, K. K. Meng, D. Pan, J. H. Zhao, and H. Z. Zheng, Adv. Mater. **24**, 4547 (2012).
[18]S. Mizukami, T. Kubota, F. Wu, X. Zhang, and T. Miyazaki, Phys. Rev. B **85**, 014416 (2012).
[19]K. Wang, E. Lu, J. W. Knepper, F. Yang, and A. R. Smith, Appl. Phys. Lett. **98**, 162507 (2011).
[20]L. J. Zhu, D. Pan, S. H. Nie, J. Lu, and J. H. Zhao, Appl. Phys. Lett. **102**, 132403 (2013).
[21]A. Köhler, I. Knez, D. Ebke, C. Felser, and S. S. P. Parkin, Appl. Phys. Lett. **103**, 162406 (2013).
[22]K. Rode, N. Baadji, D. Betto, Y. C. Lau, H. Kurt, M. Venkatesan, P. Stamenov, S. Sanvito, J. M. D. Coey, E. Fonda, E. Otero, F. Choueikani, P. Ohresser, F. Porcher, and G. André, Phys. Rev. B **87**, 184429 (2013).
[23]M. Y. Li, X. Jiang, M. G. Samant, C. Felser, and S. P. Parkin, Appl. Phys. Lett. **103**, 032410 (2013).
[24]L. J. Zhu and J. H. Zhao, Appl. Phys. A **111**, 379 (2013).
[25]F. Wu, S. Mizukami, D. Watanabe, H. Naganuma, M. Oogane, Y. Ando, and T. Miyazaki, Appl. Phys. Lett. **94**, 122503 (2009).
[26]F. Wu, S. Mizukami, D. Watanabe, E. R. Sajitha, H. Naganuma, M. Oogane, Y. Ando, and T. Miyazaki, IEEE Trans. Magn. **46**, 1863 (2010).
[27]T. A. Bither and W. H. Cloud, J. Appl. Phys. **36**, 1501 (1965).
[28]S. S. P. Parkin, M. Hayashi, and L. Thomas, Science **320**, 190 (2008).
[29]Z. X. Yang, J. Li, D. S. Wang, K. M. Zhang, and X. Xie, J. Magn. Magn. Mater. **182**, 369 (1998).
[30]W. Wang, H. Sukegawa, R. Shan, S. Mitani, and K. Inomata, Appl. Phys. Lett. **95**, 182502 (2009).
[31]O. Gutfleisch, M. A. Willard, E. Brück, C. H. Chen, S. G. Sankar, and J. P. Liu, Adv. Mater. **23**, 821 (2011).
[32]C. M. Wang, T. C. Kaspar, V. Shutthanandan, A. G. Joly, and R. J. Kurtz, Acta Mater. **59**, 4274 (2011).
[33]J. M. Hartmann, A. M. Papon, V. Destefanis, and T. Billon, J. Cryst. Growth **310**, 5287 (2008).
[34]J. Tersoff and F. K. LeGoues, Phys. Rev. Lett. **72**, 3570 (1994).
[35]H. Chen, Y. K. Li, C. S. Peng, H. F. Liu, Y. L. Liu, Q. Huang, J. M. Zhou, and K. Q. Xue, Phys. Rev. B **65**, 233303 (2002).
[36]A. G. Cervantesa, Z. Álvareza, M. López-López, A. P. Pedrazab, C. Guarnerosc, and V. M. S. Resrneroc, Appl. Surf. Sci. **258**, 1267 (2011).
[37]J. A. Cape and G. Lehman, J. Appl. Phys. **42**, 5732 (1971).
[38]M. Hehn, S. Padovani, K. Ounadjela, and J. P. Bucher, Phys. Rev. B **54**, 3428 (1996).
[39]J. U. Thiele, L. Folks, M. F. Toney, and D. K. Weller, J. Appl. Phys. **84**, 5686 (1998).
[40]C. Kooy and U. Enz, Philips Res. Rep. **15**, 7 (1960).